Cite this article as: Masunaga S, Sakurai Y, Tanaka H, Hirayama R, Matsumoto Y, Uzawa A, et al. Radiosensitivity of pimonidazole-unlabelled intratumour quiescent cell population to γ-rays, accelerated carbon ion beams and boron neutron capture reaction. Br J Radiol 2013;86:20120302.

Radiosensitivity of pimonidazole-unlabelled intratumour quiescent cell population to γ-rays, accelerated carbon ion beams and boron neutron capture reaction

[1]S MASUNAGA, MD, PhD, [2]Y SAKURAI, PhD, [2]H TANAKA, PhD, [3]R HIRAYAMA, PhD, [3]Y MATSUMOTO, PhD, [3]A UZAWA, PhD, [1]M SUZUKI, MD, PhD, [1]N KONDO, MD, PhD, [1]M NARABAYASHI, MD, PhD, [2]A MARUHASHI, PhD and [1]K ONO, MD, PhD

[1]*Particle Radiation Oncology Research Center, Research Reactor Institute, Kyoto University, Osaka, Japan,* [2]*Radiation Medical Physics, Research Reactor Institute, Kyoto University, Osaka, Japan, and* [3]*Research Center for Charged Particle Therapy, National Institute of Radiological Sciences, Chiba, Japan*

Objective: To detect the radiosensitivity of intratumour quiescent (Q) cells unlabelled with pimonidazole to accelerated carbon ion beams and the boron neutron capture reaction (BNCR).
Methods: EL4 tumour-bearing C57BL/J mice received 5-bromo-2′-deoxyuridine (BrdU) continuously to label all intratumour proliferating (P) cells. After the administration of pimonidazole, tumours were irradiated with γ-rays, accelerated carbon ion beams or reactor neutron beams with the prior administration of a ^{10}B-carrier. Responses of intratumour Q and total (P+Q) cell populations were assessed based on frequencies of micronucleation and apoptosis using immunofluorescence staining for BrdU. The response of pimonidazole-unlabelled tumour cells was assessed by means of apoptosis frequency using immunofluorescence staining for pimonidazole.
Results: Following γ-ray irradiation, the pimonidazole-unlabelled tumour cell fraction showed significantly enhanced radiosensitivity compared with the whole tumour cell fraction, more remarkably in the Q than total cell populations. However, a significantly greater decrease in radiosensitivity in the pimonidazole-unlabelled cell fraction, evaluated using a delayed assay or a decrease in radiation dose rate, was more clearly observed among the Q than total cells. These changes in radiosensitivity were suppressed following carbon ion beam and neutron beam-only irradiaton. In the BNCR, the use of a ^{10}B-carrier, especially L-*para*-boronophenylalanine-^{10}B, enhanced the sensitivity of the pimonidazole-unlabelled cells more clearly in the Q than total cells.
Conclusion: The radiosensitivity of the pimonidazole-unlabelled cell fraction depends on the quality of radiation delivered and characteristics of the ^{10}B-carrier used in the BNCR.
Advances in knowledge: The pimonidazole-unlabelled subfraction of Q tumour cells may be a critical target in tumour control.

Received 7 June 2012
Revised 25 July 2012
Accepted 4 September 2012

DOI: 10.1259/bjr.20120302

Human solid tumours are thought to contain moderately large fractions of quiescent (Q) tumour cells, which are not involved in the cell cycle and have stopped dividing, but which are as viable as established experimental animal tumour lines [1]. The presence of Q cells is probably due, at least in part, to hypoxia and the depletion of nutrition in the tumour core as a consequence of poor vascular supply [1]. As a result, with the exception of non-viable Q cells at the very edge of the necrotic rim where there is diffusion-limited hypoxia, Q cells are viable and clonogenic, but have ceased dividing.

Address correspondence to: Dr Shin-ichiro Masunaga, Particle Radiation Oncology Research Center, Research Reactor Institute, Kyoto University, 2-1010, Asashiro-nichi, Kumatori-cho, Sennan-gun, Osaka 590-0494, Japan. E-mail: smasuna@rri.kyoto-u.ac.jp
This study was supported in part by a Grant-in-aid for Scientific Research (B) (23300348, 23390355) from the Japan Society for the Promotion of Science.

Using our method for selectively detecting the response of Q cells in solid tumours to treatment that damages DNA, the Q cell population in solid tumours has been shown to exhibit more resistance to conventional radiotherapy and chemotherapy [2]. The Q cell population has also been demonstrated to have greater capacity to recover from radiotherapeutic and chemotherapeutic agent-induced damage and to have a significantly larger hypoxic fraction (HF) irrespective of the *p53* status of tumour cells [2]. However, the Q cell population in solid tumours has never been shown to be fully hypoxic [2]. Actually, the size of the HF of Q cell populations in SCC VII squamous cell carcinomas, implanted in the hind legs of C3H/He mice and with a diameter of 1 cm, was $55.1 \pm 6.2\%$ (mean ± standard error) [3]. Thus, this value was significantly less than 100%, indicating that the Q cell population undoubtedly includes oxygenated tumour cells.

A few years ago, the universal detection of hypoxic cells in both tissues and cell cultures became possible using pimonidazole (a substituted 2-nitroimidazole) and a mouse immunoglobulin (Ig)G1 monoclonal antibody (MAb1) to stable covalent adducts formed through reductive activation of pimonidazole in hypoxic cells [4]. Here, we tried to selectively detect the response of the pimonidazole-unlabelled and probably oxygenated cell fraction of the Q cell population. To achieve this we combined our method for selectively detecting the response of Q cells in solid tumours with the method for detecting cell and tissue hypoxia using pimonidazole and MAb1 to pimonidazole.

High-linear energy transfer (LET) radiation including neutrons is more effective [2] than low-LET X- or γ-radiation at inducing biological damage. High-LET radiation shows a higher relative biological effectiveness (RBE) value for cell killing, a reduced oxygen effect and a reduced dependence on the cell cycle [2, 5], making it potentially superior to low-LET radiation in the treatment of malignant tumours. Reactor thermal and epithermal neutron beams available at our institute had been also shown to have a significantly higher RBE value than γ-rays in irradiated tumour cells *in vivo* [2]. Owing to a selective physical dose distribution and enhanced biological damage in target tumours, particle radiation therapy with protons or heavy ions has gained increasing interest worldwide, and many clinical centres are considering introducing radiation therapy with charged particles. However, almost all reports on the biological advantages of charged particle beams are based on effects only on total tumour cell populations as a whole using *in vitro* cell cultures or *in vivo* solid tumours [1, 5].

Intensity-modulated radiotherapy and stereotactic irradiation have become common as new radiotherapy modalities for the treatment of malignancies. These techniques often require precise positioning of patients and longer exposure times in a single treatment session [6, 7]. Prolongation of irradiation time may induce adverse radiation effects and evokes major concern related to the dose-rate effect. Thus, there is a need to clarify the effect of a reduction in dose rate on the radiosensitivity of tumours *in vivo*.

In the present study, the radiosensitivity of the pimonidazole-unlabelled cell fraction of the Q cell population, following cobalt-60 γ-ray or 290 MeV u^{-1} accelerated carbon ion beam irradiation at both a high dose rate (HDR) and a reduced dose rate (RDR), was determined, compared with irradiation using reactor thermal neutron beams following the administration of a ^{10}B-carrier at our institute. This is the first attempt to evaluate the sensitivity of oxygenated fractions of Q tumour cells *in vivo* in response to particle radiation.

Methods

Mice and tumours

EL4 lymphoma cells (Cell Resource Center for the Biomedical Research Institute of Development, Aging and Cancer, Tohoku University, Japan) derived from C57BL/6J mice were maintained *in vitro* in RPMI 1640 medium supplemented with 12.5% foetal bovine serum. The *p53* status of the EL4 tumour cells was the wild type [8]. Cells were collected from exponentially growing cultures and approximately 1.0×10^5 tumour cells were inoculated subcutaneously into the left hind legs of 9-week-old syngeneic female C57BL/6J mice (Japan Animal Co. Ltd, Osaka, Japan). 14 days after the inoculation, the tumours, approximately 1 cm in diameter, were employed for irradiation in this study, and the body weight of the tumour-bearing mice was 22.1 ± 2.3 g. Mice were handled according to the Recommendations for Handling of Laboratory Animals for Biomedical Research, compiled by the Committee on Safety Handling Regulations for Laboratory Animal Experiments.

Labelling with 5-bromo-2′-deoxyuridine

9 days after the tumour inoculation, mini-osmotic pumps (Durect Corporation, Cupertino, CA) containing 5-bromo-2′-deoxyuridine (BrdU) dissolved in physiological saline (250 mg ml^{-1}) were implanted subcutaneously to enable the labelling of all P cells over a 5-day period [9]. The percentage of labelled cells after continuous labelling with BrdU was $66.1\pm3.8\%$ and plateau at this stage. Therefore, tumour cells not incorporating BrdU after continuous exposure were regarded as Q cells.

Treatment

After the labelling with BrdU, tumour-bearing mice received an intraperitoneal administration of pimonidazole hydrochloride (Hypoxyprobe Inc., Burlington, MA) dissolved in physiological saline at a dose of 60 mg kg^{-1}. 90 min later, mice received γ-ray or accelerated carbon ion beam irradiation, or reactor neutron beam irradiation following administration of the ^{10}B-carrier with no anaesthetic.

γ-rays were delivered using a cobalt-60 γ-ray irradiator at dose rates of 2.500 and 0.039 Gy min^{-1} representing HDR and RDR irradiation, respectively. Carbon-12 ions were accelerated up to 290 MeV u^{-1} by the synchrotron of the heavy ion medical accelerator installed at the National Institute of Radiological Sciences in Chiba, Japan. The dose rate was regulated through a beam attenuation system, and irradiation was conducted using horizontal carbon beams with a dose rate of 1.000 or 0.035 Gy min^{-1}. The LET of a carbon ion beam with a 6-cm spread-out Bragg peak (SOBP) ranges from 14 keV μm^{-1} to >200 keV μm^{-1}, depending on depth. The desired LET beam was obtained by selecting the depth along the beam path using a Lucite range shifter. An LET of 50 keV μm^{-1} at the middle of the SOBP was employed here.

Sodium mercaptoundecahydrododecaborate-^{10}B (sodium borocaptate-^{10}B; BSH; $Na_2{}^{10}B_{12}H_{11}SH$; 125 mg kg^{-1}) and boronophenylalanine-^{10}B (BPA; $C_9H_{12}{}^{10}BNO_4$; 250 mg kg^{-1}) were purchased from KatChem Ltd (Rez, Czech Republic) and prepared freshly by dissolving in physiological saline, and injected intraperitoneally in a volume of 0.02 ml g^{-1} mouse body weight. In accordance with our previous study [10], at a dose of <500 mg kg^{-1}

for BSH and $<1500\,mg\,kg^{-1}$ for BPA, no apparent toxicity was observed. Based on the certificate of analysis and material safety data sheet provided, BSH was not contaminated with the borocapatate dimer (BSSB, $[^{10}B_{24}H_{22}S_2]^{4-}$). Since the intratumour ^{10}B concentration during neutron irradiation is a crucial determinant of the cell-kill effect in the boron neutron capture reaction (BNCR), to obtain similar intratumour ^{10}B concentrations during exposure to the neutron beam, irradiation was started at selected time points after the intraperitoneal injection of the ^{10}B-carriers at a selected dose of ^{10}B. Based on a preliminary study of the biodistribution of ^{10}B, irradiation was started from 45 min after the intraperitoneal injection of 125 and 250 mg kg^{-1} (71.0 and 12.0 mg $^{10}B\,kg^{-1}$) of BSH and BPA, respectively. ^{10}B concentrations were determined with a thermal neutron guide tube installed at the Kyoto University research reactor (KUR) [11].

The tumour-bearing mice were irradiated with a reactor neutron beam at a power of 1 MW at KUR. A lithium fluoride (LiF) thermoplastic shield was employed to avoid irradiating other body parts except implanted solid tumours. Neutron irradiation was performed using a reactor neutron beam with a cadmium ratio of 9.4. The cadmium ratio is the ratio of the response of an uncovered neutron detector to that of the same detector under identical conditions when it is covered with cadmium of a specified thickness. The neutron fluence was measured from the radioactivation of gold foil at both the front and back of the tumours. Since the tumours were small and located just beneath the surface, the neutron fluence was assumed to decrease linearly from the front to back of the tumours. Thus, we used the average neutron fluence determined from the values measured at the front and back. Contaminating γ-ray doses including secondary γ-rays were measured with a thermoluminescence dosemeter (TLD) powder at the back of the tumours. The TLD used was beryllium oxide (BeO) enclosed in a quartz glass capsule. BeO itself has some sensitivity to thermal neutrons. The thermal neutron fluence of $8\times10^{12}\,cm^{-2}$ is equal to an approximately 1-cGy γ-ray dose. We usually use the TLD together with gold activation foil for the neutron-sensitivity correction. The details have been described previously [12]. For the estimation of neutron energy spectra, eight kinds of activation foil and 14 kinds of nuclear reaction were used [12]. The absorbed dose was calculated using the flux-to-dose conversion factor [13]. The tumours contained H (10.7% in terms of weight), C (12.1%), N (2%), O (71.4%) and others (3.8%) [14]. The average neutron flux and Kerma rate of the employed beam were $1.0\times10^{9}\,n\,cm^{-2}\,s^{-1}$ and $48.0\,cGy\,h^{-1}$ for the thermal neutron range (<0.6 eV), $1.6\times10^{8}\,n\,cm^{-2}\,s^{-1}$ and $4.6\,cGy\,h^{-1}$ for the epithermal neutron range (0.6–10.0 keV), and $9.4\times10^{6}\,n\,cm^{-2}\,s^{-1}$ and $32.0\,cGy\,h^{-1}$ for the fast neutron range (>10 keV), respectively. The Kerma rate for the boron dose per $\Phi\,n\,cm^{-2}\,s^{-1}$ of thermal neutron flux for $1\,\mu g\,g^{-1}$ of ^{10}B was $2.67\times10^{-8}\,\Phi\,cGy\,h^{-1}$. The contaminating γ-ray dose rate was $66.0\,cGy\,h^{-1}$.

Individual animals were secured in a specially designed device made of acrylic resin with the tail firmly fixed in position with adhesive tape. Each treatment group also included mice that had not been pretreated with BrdU.

Immunofluorescence staining of BrdU-labelled and/or pimonidazole-labelled cells, and observation of apoptosis and micronucleation

Based on our previous report related to the determination of the timing of apoptosis [10], as an immediate assay, an apoptosis assay was undertaken at 6 h after irradiation and a micronucleus assay was carried out immediately after irradiation. Tumours were excised from mice given BrdU, weighed, minced and trypsinised: 0.05% trypsin and 0.02% ethylenediamine-tetraacetic acid (EDTA) in phosphate-buffered saline (PBS) at 37°C for 20 min. Furthermore, as a delayed assay, tumours were also excised from mice given BrdU, weighed, minced and trypsinised at 30 h after irradiation for the apoptosis assay, and at 24 h after irradiation for the micronucleus assay. For the apoptosis assay, single cell suspensions were fixed without further treatment. For the micronucleus assay, tumour cell suspensions were incubated for 72 h in tissue culture dishes containing complete culture medium and $1.0\,\mu g\,ml^{-1}$ of cytochalasin-B, to inhibit cytokinesis while allowing nuclear division. The cultures were then trypsinised and cell suspensions were fixed. For both assays, after the centrifugation of fixed cell suspensions, the cell pellet was resuspended with cold Carnoy's fixative (ethanol–acetic acid=3:1 in volume). The suspension was placed on a glass microscope slide and the sample was dried at room temperature. Slides were treated with 2 M hydrochloric acid for 60 min at room temperature to dissociate the histones and partially denature the DNA. They were then immersed in borax-borate buffer (pH 8.5) to neutralise the acid. BrdU-labelled tumour cells were detected using indirect immunofluorescence staining with a rat monoclonal anti-BrdU antibody (Abcam plc, Cambridge, UK) and a goat Alexa Fluor 488-conjugated anti-rat IgG antibody (Invitrogen Corp., Carlsbad, CA). Pimonidazole-labelled tumour cells were detected using indirect immunofluorescence staining with a mouse monoclonal anti-pimonidazole antibody (Hypoxyprobe Inc.) and a rabbit Alexa Fluor 594-conjugated anti-mouse IgG antibody (Invitrogen Corp.). To enable the observation of the triple staining of tumour cells with green-emitting Alexa Fluor 488 and red-emitting Alexa Fluor 594, cells on the slides were treated with blue-emitting 4′6-diamidino-2-phenylindole (DAPI; $0.5\,\mu g\,ml^{-1}$ in PBS) and imaged using a fluorescence microscope.

The frequency of apoptosis in cells not labelled with BrdU (=Q cells at irradiation) and tumour cells not labelled with pimonidazole was determined by counting apoptotic cells in tumour cells that did not show green fluorescence from Alexa Fluor 488 and red fluorescence from Alexa Fluor 594, respectively. The apoptosis frequency was defined as the ratio of the number of apoptotic cells to the total number of observed tumour cells [10]. The micronucleus frequency in BrdU-unlabelled cells was examined by counting the micronuclei in the binuclear cells that did not show green fluorescence emitted by Alexa Fluor 488. The micronucleus frequency was defined as the ratio of the number of micronuclei in the binuclear cells to the total number of binuclear cells observed [2].

The ratios obtained in tumours not pre-treated with BrdU indicated the apoptosis frequency and the micronucleus frequency in the total (P+Q) tumour cell

populations. >300 tumour cells and binuclear cells were counted to determine the apoptosis frequency and the micronucleus frequency, respectively.

Clonogenic cell survival assay

The clonogenic cell survival assay was also performed in mice given no BrdU or pimonidazole using an *in vivo–in vitro* assay method. Tumours were disaggregated by stirring for 20 min at 37°C in PBS containing 0.05% trypsin and 0.02% EDTA. The cell yield was $(1.1 \pm 0.3) \times 10^8\ g^{-1}$ tumour weight. A colony formation assay using the *in vivo–in vitro* assay method was performed with the culture medium mixed with methylcellulose ($15.0\ g\ l^{-1}$; Aldrich, Milwaukee, WI).

The apoptosis and micronucleus frequencies and surviving fractions for the total cell population were obtained from cells in tumours that were not pre-treated with BrdU or pimonidazole. The apoptosis and micronucleus frequencies for Q cells were obtained from unlabelled tumour cells after continuous BrdU labelling without pimonidazole loading. The apoptosis frequencies for the total tumour cell populations that were not labelled with pimonidazole were obtained from tumour cells that were not labelled with pimonidazole after pimonidazole loading without BrdU pre-treatment. The apoptosis frequencies for Q cells that were not labelled with pimonidazole were obtained from tumour cells that were not labelled with BrdU or pimonidazole after both continuous BrdU labelling and pimonidazole loading. Thus, there was no effect of interaction between BrdU and irradiation or between pimonidazole and irradiation on the values for the apoptosis and micronucleus frequencies and surviving fractions. Incidentally, since the rate of pimonidazole-labelled tumour cells could change during culturing with cytochalasin-B over 3 days, following the production of single tumour cell suspensions by excising and mincing the tumours from mice that underwent pimonidazole loading, the micronucleus frequency for the cell fraction that was not labelled with pimonidazole after pimonidazole loading was not determined. As a consequence, the radiosensitivity of the pimonidazole-unlabelled cell fractions was only determined in relation to apoptosis induction. This was the reason for using the EL4 leukaemia cell line with its much greater capacity for the induction of apoptosis than other solid tumour-originating cell lines [10].

Data analysis and statistics

More than three tumour-bearing mice were used to assess each set of conditions and each experiment was repeated at least twice. To examine the differences between pairs of values, Student's *t*-test was used when variances of the two groups were assumed to be equal with the Shapiro–Wilk normality test; otherwise the Welch *t*-test was used.

Results

The plating efficiency and the micronucleus and apoptosis frequencies after a radiation dose of 0 Gy are shown in Table 1. The micronucleus and apoptosis frequencies were significantly higher for the Q cell population than for the total cell population. In contrast, the apoptosis frequency was significantly lower for the cell fraction that was not labelled with pimonidazole than for the whole tumour cell fraction in both the Q and total tumour cell populations.

Cell survival curves for the total tumour cell population as a function of radiation dose are shown in Figure 1. In the irradiation of γ-rays and carbon ion beams, the surviving fractions (SFs) increased in the following order, with a more remarkable change for γ-rays than carbon ion beams: immediately after HDR irradiation; 24 h after HDR irradiation; immediately after RDR irradiation. In the BNCR, the SFs increased as follows: with BPA; with BSH; without a ^{10}B-carrier.

For baseline correction, we used the net micronucleus frequency to exclude the micronucleus frequency in non-irradiated tumours. The net micronucleus frequency was defined as the micronucleus frequency in the irradiated tumours minus the micronucleus frequency in the non-irradiated tumours. Dose–response curves for the net micronucleus frequency in total and Q tumour cell populations as a function of radiation dose are shown in Figure 2. Overall, the net micronucleus frequencies were significantly lower in the Q cells than in the total cell population. In both the total and Q cell populations after the irradiation of γ-rays and carbon ion beams, the net micronucleus frequencies decreased as follows, with a more remarkable change for γ-rays than carbon ion beams: immediately after HDR irradiation; 24 h after HDR irradiation; immediately after RDR irradiation. In the BNCR, the net micronucleus frequencies for the total cell population increased in the following order: without a ^{10}B-carrier; with BSH; with BPA. However, those for the Q cell population increased in the following order: without a ^{10}B-carrier; with BPA; with BSH.

For another baseline correction, we used the net apoptosis frequency to exclude the apoptosis frequency in non-irradiated tumours. The net apoptosis frequency was the apoptosis frequency in the irradiated tumours minus that in the non-irradiated tumours. Dose–response curves for the net apoptosis frequency in the total and Q tumour cell populations as a function of radiation dose are shown in Figure 3. Overall, the net apoptosis frequencies were significantly lower in the Q than in the total cell population, with much larger differences for γ-rays than for carbon ion beams. Moreover, the net apoptosis frequency was significantly higher for the cell fraction that was not labelled with pimonidazole than for the whole tumour cell fraction in both the Q and total cell populations under each set of

Table 1. Plating efficiency and micronucleus frequency at 0 Gy

Parameter	Total tumour cells	Quiescent cells
Plating efficiency (%)	25.5 ± 6.8[a]	–
Micronucleus frequency	0.053 ± 0.003	0.073 ± 0.006
Apoptosis frequency		
In whole cell fraction	0.040 ± 0.001	0.067 ± 0.004
In pimonidazole unlabelled cell fraction	0.017 ± 0.001	0.028 ± 0.003

[a]Mean ± standard error (n=9).

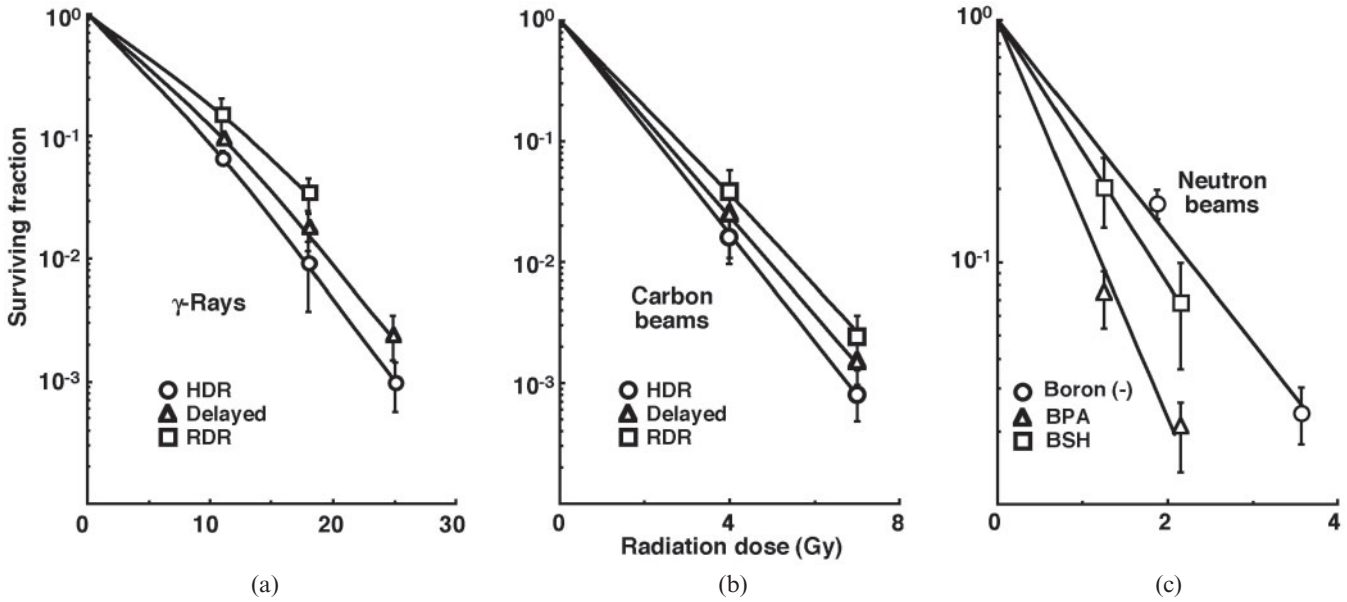

Figure 1. Cell survival curves for the whole tumour cell fraction in the total tumour cell population of EL4 tumours as a function of (a) γ-ray, (b) accelerated carbon ion beam or (c) reactor neutron beam radiation dose. Circles, triangles and squares represent the surviving fractions immediately after high dose rate (HDR) and at 24 h after (delayed) HDR and reduced dose-rate (RDR) γ-ray or accelerated carbon ion beam irradiation, respectively. For reactor neutron beam irradiation, circles, triangles and squares represent the surviving fractions for without a ^{10}B-carrier [boron (–)], with boronophenylalanine-^{10}B (BPA) and with sodium mercaptoundecahydrododecaborate-^{10}B (BSH), respectively. Bars represent standard errors (n=9).

conditions, again with a much larger difference for γ-rays than for carbon ion beams. For both the pimonidazole-unlabelled and the whole cell fractions, in the Q as well as total tumour cell population, the net apoptosis frequencies decreased as follows, with a more remarkable change for γ-rays than carbon ion beams: immediately after HDR irradiation; 24 h after HDR irradiation; immediately after RDR irradiation. Also in the BNCR, the pimonidazole-unlabelled cells showed higher net apoptosis frequencies than the whole tumour cell fractions with little remarkable change in the Q compared with the total cell population and with increased

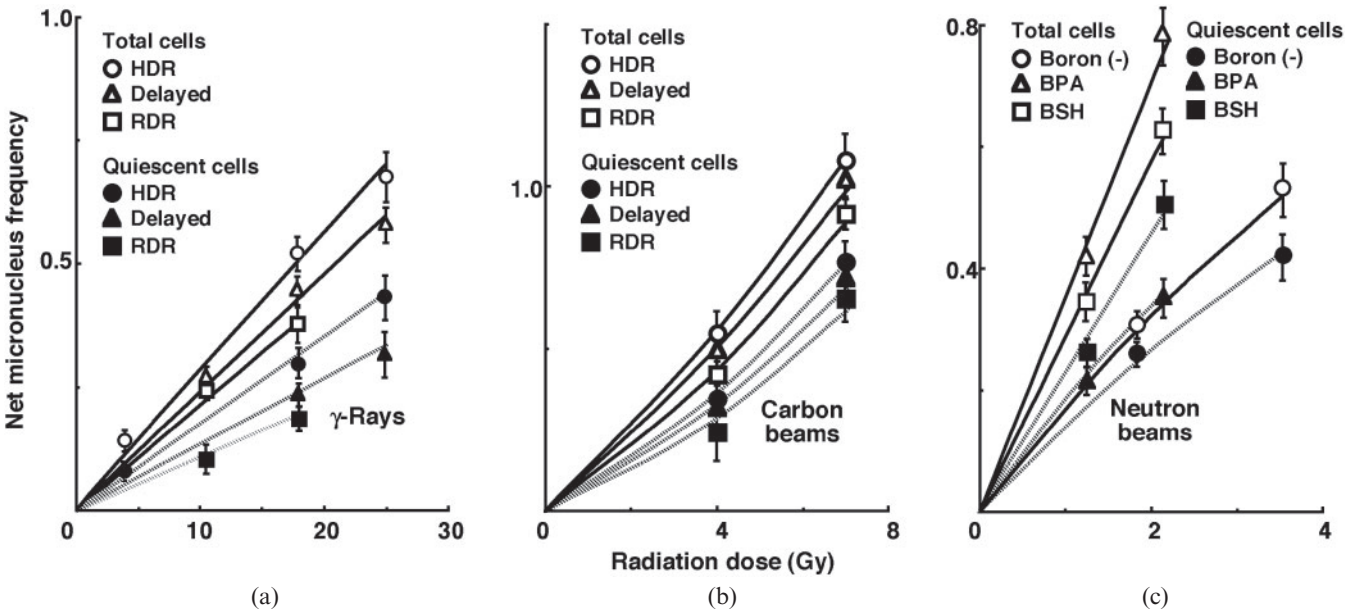

Figure 2. Dose–response curves of the net micronucleus frequency for the whole tumour cell fraction in the total and quiescent (Q) tumour cell populations of EL4 tumours as a function of (a) γ-ray, (b) accelerated carbon ion beam or (c) reactor neutron beam radiation dose. Open and solid symbols represent the net micronucleus frequencies for total and Q tumour cell populations, respectively. Circles, triangles and squares represent the net micronucleus frequencies immediately after high dose rate (HDR) and at 24 h after (delayed) HDR and reduced dose-rate (RDR) γ-ray or accelerated carbon ion beam irradiation, respectively. For reactor neutron beam irradiation, circles, triangles and squares represent the net micronucleus frequencies for without a ^{10}B-carrier [boron (–)], with boronophenylalanine-^{10}B (BPA) and with sodium mercaptoundecahydrododecaborate-^{10}B (BSH), respectively. Bars represent standard errors (n=9).

change in the following order: without a ^{10}B-carrier; with BSH; with BPA.

To evaluate the radiosensitivity of the cell fraction that was not labelled with pimonidazole, as compared with the whole cell fraction in both the total and Q cell populations, dose-modifying factors (DMFs) were calculated using the data obtained under γ-ray and carbon ion beam irradiation conditions (Figure 3, Table 2). Overall, DMF values tended to be higher for the Q cell than total cell population, and in particular immediately after HDR irradiation, with a much larger difference for γ-rays than carbon ion beams. In the total cell population, the DMF values were almost constant. However, for Q cells, the DMF values had a tendency to decrease as follows: immediately after HDR irradiation; 24 h after HDR irradiation; immediately after RDR irradiation. Also in the BNCR (Table 3), DMF values tended to be higher for the Q cell than total cell population, and in both Q and total cell populations, the DMF values had a tendency to increase in the following order: without a ^{10}B-carrier; with BSH; with BPA.

To investigate the reduction in radiosensitivity caused by a delayed assay or a decrease in the radiation dose rate, DMFs were calculated using the data for γ-ray and carbon ion beam irradiation conditions given in Figures 1–3 (Table 4). Overall, carbon beams showed lower DMF values than γ-rays under all sets of conditions. On the whole, in the fraction unlabelled with pimonidazole or the whole cell fraction, the values were higher after RDR irradiation than at 24 h after HDR irradiation in both the total and Q cell populations, particularly in the latter population. The DMF values were significantly higher in the Q cell than total cell population in both the pimonidazole-unlabelled and whole cell fractions. In both the Q and total cell populations, the values were higher for pimonidazole-unlabelled cell fractions than whole cell fractions, particularly in the case of the Q cells.

To estimate the radio-enhancing effect of ^{10}B-carriers, irradiation with BPA and BSH in the total and Q cell populations was compared with neutron beam irradiation only, using the data shown in Figures 1–3 (Table 5). Both BPA and BSH enhanced the sensitivity of the total cell population significantly more than that of the Q cell population. Further, BPA tended to affect the total cell population more than did BSH. In contrast, the sensitivity of Q cells was relatively more enhanced with BSH than BPA. In both the Q and total cell populations, but especially in Q cells, the values were higher for pimonidazole-unlabelled cell fractions than whole cell fractions.

To examine the difference in radiosensitivity between the total and Q cell populations, DMFs that allow us to compare the dose of radiation necessary to obtain each end point in the two cell populations were calculated using the data in Figures 2 and 3 (Tables 6 and 7). All DMF values were significantly higher than 1.0, and carbon beams showed smaller values than γ-rays under

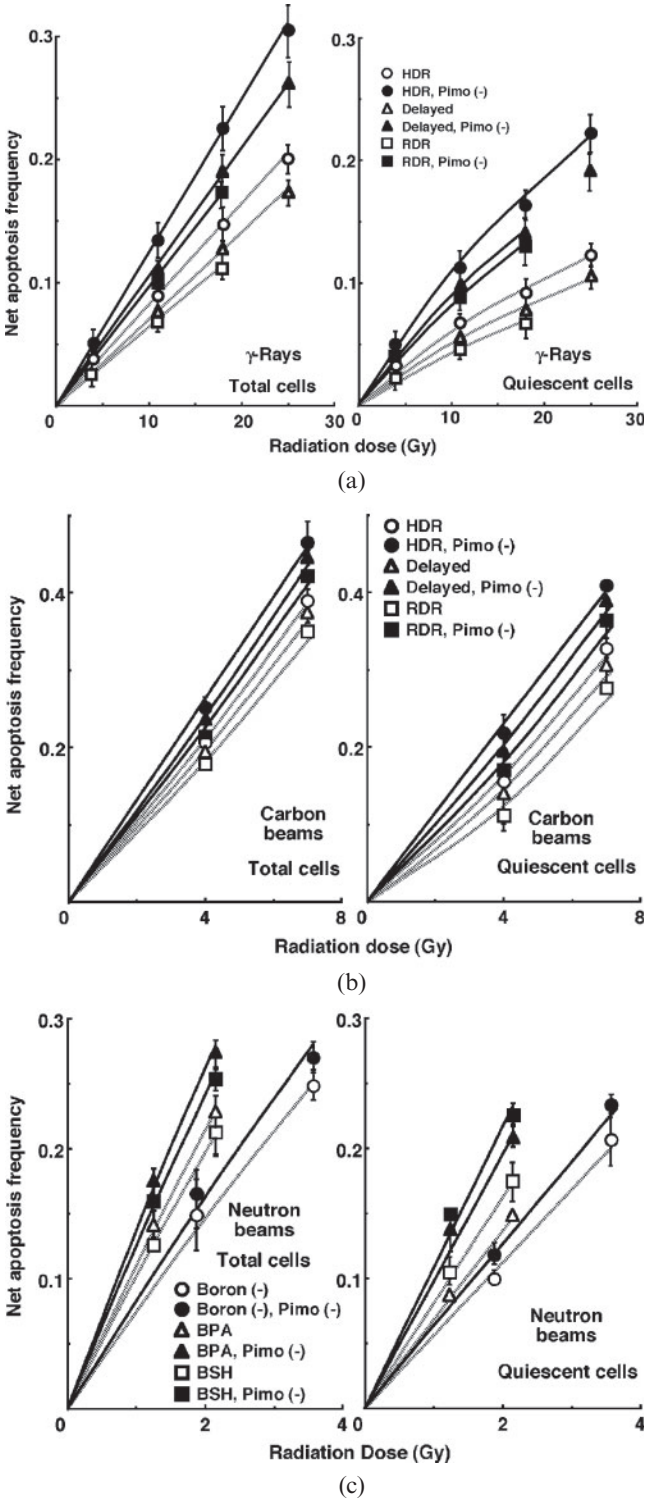

Figure 3. Dose–response curves for the net apoptosis frequency of the total (left panel) and quiescent (Q) (right panel) tumour cell populations of EL4 tumours as a function of (a) γ-ray, (b) accelerated carbon ion beam or (c) reactor neutron beam radiation dose. Open and solid symbols represent the net apoptosis frequencies for the whole tumour cell fraction and the cell fraction not labelled with pimonidazole [pimo (–)] in both the total and Q tumour cell populations, respectively. Circles, triangles and squares represent the net apoptosis frequencies immediately after high dose rate (HDR) and at 24 h after (delayed) HDR and reduced dose-rate (RDR) γ-ray or accelerated carbon ion beam irradiation, respectively. For reactor neutron beam irradiation, circles, triangles and squares represent the net apoptosis frequencies for without a ^{10}B-carrier [boron (–)], with boronophenylalanine-^{10}B (BPA) and with sodium mercaptoundecahydrododecaborate-^{10}B (BSH), respectively. Bars represent standard errors (n=9).

Table 2. Dose-modifying factors for the pimonidazole-unlabelled cell fraction as compared with the whole cell fraction in the total or quiescent cell population[a]

Parameter	High dose rate: immediately after	High dose rate: 24 h after	Reduced dose rate
Net apoptosis frequency=0.06			
γ-rays			
Total cell population	1.55 (1.45–1.65)[b]	1.5 (1.4–1.6)	1.5 (1.4–1.6)
Quiescent cell population	1.7 (1.5–1.9)	1.65 (1.55–1.75)	1.6 (1.5–1.7)
Carbon beams			
Total cell population	1.25 (1.1–1.4)	1.2 (1.1–1.3)	1.2 (1.1–1.3)
Quiescent cell population	1.6 (1.5–1.7)	1.5 (1.4–1.6)	1.4 (1.3–1.5)

[a]The ratio of the dose of radiation necessary to obtain each end point in a whole cell fraction to that needed to obtain each end point in the pimonidazole-unlabelled cell fraction.
[b]Values in parentheses are 95% confidence limits, determined using standard errors. When the ranges of 95% confidence limits showed no overlap between two values, the difference between the two values were significant ($p<0.05$) based on a χ^2 test.

each set of conditions (Table 6). The DMF values increased as follows: immediately after HDR irradiation; 24 h after HDR irradiation; immediately after RDR irradiation. The values were lower for the subpopulation that was not labelled with pimonidazole than for the whole cell population (Table 6). In the BNCR, the DMF values increased in the following order: without ^{10}B-carrier; with BSH; with BPA (Table 7). Again, the values were lower for the subpopulation not labelled with pimonidazole than for the whole cell population.

Discussion

In recent years the concept of cancer stem cells (CSCs), or tumour-initiating cells (tumour clonogens), has attracted a great deal of interest because of the potential clinical significance [15]. In part, these cells are thought to exist in a pathophysiological microenvironment where hypoxia, low pH and nutrient deprivation occur. Under these microenvironmental conditions, dividing tumour cells have also been thought to become quiescent. Actually, a subset of CSCs or tumour clonogens consists of non-dividing quiescent cells [16]. Thus, in the current study we tried to clarify the radiobiological characteristics of the subpopulation in the intratumour Q cell population in the context of CSC or tumour clonogen characteristices.

The fraction of cells that were not labelled with pimonidazole showed significantly higher radiosensitivity than the whole cell fraction in both the Q and total cell populations, and among the Q cells in particular (Table 2). This was probably because the pimonidazole-unlabelled cells were more oxygenated than the whole cell fraction, which comprised oxygenated and hypoxic tumour cells, in both the Q and total tumour cell populations [4]. Additionally, the Q cell population as a whole included a larger HF than the total tumour cell population [2]. As shown in Table 4, the pimonidazole-unlabelled cell fraction had a greater recovery capacity than the whole cell fraction, especially in the case of the Q cells. The radiosensitivity decreased in the following order: immediately after HDR irradiation, at 24 h after HDR irradiation and immediately after RDR irradiation, particularly in the Q cells (Table 4). As a consequence, in the case of the Q cells, the difference in radiosensitivity between the pimonidazole-unlabelled and whole cell fractions declined in the same order (Table 2). One mechanism of CSC or tumour clonogen resistance to cytotoxic treatment is supposed to be based on an enhanced DNA repair capacity [17]. Here, the pimonidazole-unlabelled Q cell fraction showed a much greater recovery capacity than the Q cell population as a whole, even if the recovery capacity was significantly greater in the entire Q cell population than in the total tumour cell population as a whole. In other words, from the viewpoint of not only quiescent status but also enhanced DNA repair capacity, the characteristics of the pimonidazole-unlabelled cell fraction in the Q cell population were found to be similar to those of CSCs or tumour clonogens.

The microenvironmental conditions under which dividing tumour cells become quiescent might promote the formation of micronuclei and apoptosis at 0 Gy in the whole Q tumour cell fractions, partly due to hypoxic stress (Table 1) [1]. In this study, the Q cells were shown to be significantly less radiosensitive and to have a greater recovery capacity than the total cell population

Table 3. Dose-modifying factors for the pimonidazole-unlabelled cell fraction as compared with the whole cell fraction in the total or quiescent cell population[a]

Parameter	Neutrons only	With BPA	With BSH
Net apoptosis frequency=0.06			
Neutron beams			
Total cell population	1.1 (1.0–1.2)[b]	1.3 (1.2–1.4)	1.25 (1.15–1.35)
Quiescent cell population	1.15 (1.05–1.25)	1.45 (1.3–1.6)	1.35 (1.25–1.45)

BPA, boronophenylalanine-^{10}B; BSH, sodium mercaptoundecahydrododecaborate-^{10}B.
[a]The ratio of the dose of radiation necessary to obtain each end point in a whole cell fraction to that needed to obtain each end point in the pimonidazole-unlabelled cell fraction.
[b]Values in parentheses are 95% confidence limits, determined using standard errors. When the ranges of 95% confidence limits showed no overlap between two values, the difference between the two values were significant ($p<0.05$) based on a χ^2 test.

Table 4. Dose-modifying factors obtained using a delayed assay or a reduced radiation dose rate[a]

Parameter	High dose rate: 24 h after	Reduced dose rate
Surviving fraction=0.08		
Total cells		
γ-rays	1.15 (1.1–1.2)[b]	1.4 (1.3–1.5)
Carbon beams	1.1 (1.0–1.2)	1.2 (1.1–1.3)
Net micronucleus frequency=0.2		
Total cells		
γ-rays	1.2 (1.1–1.3)	1.35 (1.25–1.45)
Carbon beams	1.05 (1.0–1.1)	1.2 (1.1–1.3)
Quiescent cells		
γ-rays	1.4 (1.3–1.5)	1.6 (1.45–1.75)
Carbon beams	1.1 (1.0–1.2)	1.25 (1.15–1.35)
Net apoptosis frequency=0.06		
Total cells		
In whole cell fraction		
γ-rays	1.15 (1.1–1.2)	1.3 (1.2–1.4)
Carbon beams	1.05 (1.0–1.2)	1.2 (1.1–1.3)
In pimonidazole-unlabelled cell fraction		
γ-rays	1.2 (1.1–1.3)	1.3 (1.2–1.4)
Carbon beams	1.05 (1.0–1.2)	1.2 (1.1–1.3)
Quiescent cells		
In whole cell fraction		
γ-rays	1.35 (1.25–1.45)	1.55 (1.45–1.65)
Carbon beams	1.15 (1.1–1.2)	1.25 (1.15–1.35)
In pimonidazole-unlabelled cell fraction		
γ-rays	1.45 (1.35–1.55)	1.65 (1.5–1.8)
Carbon beams	1.15 (1.1–1.2)	1.35 (1.25–1.45)

[a]The ratio of the dose of radiation necessary to obtain each end point with a delayed assay or reduced dose-rate irradiation to that needed to obtain each end point with an assay immediately after high dose-rate irradiation.
[b]Values in parentheses are 95% confidence limits, determined using standard errors. When the ranges of 95% confidence limits showed no overlap between two values, the difference between the two values were significant ($p<0.05$) based on a χ^2 test.

(Figures 2 and 3, Table 6). This finding indicated that more Q cells survive radiation therapy than P cells. In particular, in the cell fraction that was not labelled with pimonidazole, the difference in radiosensitivity between the Q and total cell populations was markedly increased when evaluated using the delayed assay or by employing a reduced radiation dose rate. This was due to the greater recovery capacity of the unlabelled Q cell fraction as compared with the unlabelled cell fraction in the total tumour cell population (Table 6). Therefore, whether in the pimonidazole-unlabelled or the whole Q cell population, it follows that control of the Q cells has a great impact on the outcome of radiation therapy and that the Q cell population can be a critical target in the control of solid tumours.

Table 5. Enhancement ratios[a] owing to combination with a ^{10}B-carrier

^{10}B-carrier	Total cell population	Quiescent cells
Surviving fraction=0.08		
BPA	1.95 (1.75–2.15)[b]	–
BSH	1.3 (1.2–1.4)	–
Net micronucleus frequency=0.2		
BPA	2.0 (1.8–2.2)	1.7 (1.6–1.8)
BSH	1.3 (1.2–1.4)	1.8 (1.65–1.95)
Net apoptosis frequency=0.06		
In whole cell fraction		
BPA	1.5 (1.4–1.6)	1.25 (1.15–1.35)
BSH	1.4 (1.3–1.5)	1.35 (1.2–1.5)
In pimonidazole-unlabelled cell fraction		
BPA	1.65 (1.5–1.8)	1.65 (1.5–1.8)
BSH	1.5 (1.4–1.6)	1.7 (1.6–1.8)

BPA, boronophenylalanine-^{10}B; BSH, sodium mercaptoundecahydrododecaborate-^{10}B.
[a]The ratio of the dose of radiation necessary to obtain each end point without a ^{10}B-carrier to that needed to obtain each end point with a ^{10}B-carrier.
[b]Values in parentheses are 95% confidence limits, determined using standard errors. When the ranges of 95% confidence limits showed no overlap between two values, the difference between the two values were significant ($p<0.05$) based on a χ^2 test.

At high-LET carbon ion irradiation, tumour radiosensitivity and the capacity to recover from radiation-induced damage are known to be significantly less dependent on intratumour oxygenation status and the irradiation dose rate [18]. This is thought to be partly because the frequency of closely spaced DNA lesions forming a cluster of DNA damage produced by high-LET carbon ion beams is much less dependent on oxygenation status at the time of irradiation than that of DNA damage produced by low-LET γ-ray irradiation [5, 18]. Thus, the differences in radiosensitivity, not only between total and Q cell populations but also between

Table 6. Dose-modifying factors for quiescent cells relative to total tumour cells[a]

Parameter	High dose rate: immediately after	High dose rate: 24 h after	Reduced dose rate
Net micronucleus frequency=0.2			
γ-rays	1.65 (1.5–1.8)[b]	1.8 (1.65–1.95)	1.9 (1.75–2.05)
Carbon beams	1.35 (1.25–1.45)	1.4 (1.25–1.55)	1.45 (1.3–1.6)
Net apoptosis frequency=0.06			
In whole cell fraction			
γ-rays	1.3 (1.2–1.4)	1.45 (1.35–1.55)	1.55 (1.4–1.7)
Carbon beams	1.15 (1.05–1.25)	1.25 (1.15–1.35)	1.3 (1.2–1.4)
In pimonidazole-unlabelled cell fraction			
γ-rays	1.2 (1.1–1.3)	1.4 (1.3–1.5)	1.55 (1.4–1.7)
Carbon beams	1.1 (1.0–1.2)	1.2 (1.1–1.3)	1.25 (1.15–1.35)

[a]The ratio of the dose of radiation necessary to obtain each end point in the quiescent cell population to that needed to obtain each end point in the total tumour cell population.
[b]Values in parentheses are 95% confidence limits, determined using standard errors. When the ranges of 95% confidence limits showed no overlap between two values, the difference between the two values were significant ($p<0.05$) based on a χ^2 test.

Table 7. Dose-modifying factors for quiescent cells relative to total tumour cells[a]

Parameter	Neutrons only	With BPA	With BSH
Net micronucleus frequency=0.2	1.2 (1.1–1.3)[b]	2.15 (1.9–2.4)	1.25 (1.15–1.35)
Net apoptosis frequency=0.06			
In whole cell fraction	1.3 (1.2–1.4)	1.6 (1.45–1.75)	1.25 (1.15–1.35)
In pimonidazole-unlabelled cell fraction	1.25 (1.15–1.35)	1.35 (1.2–1.5)	1.15 (1.05–1.25)

BPA, boronophenylalanine-^{10}B; BSH, sodium mercaptoundecahydrododecaborate-^{10}B.
[a]The ratio of the dose of radiation necessary to obtain each end point in the quiescent cell population to that needed to obtain each end point in the total tumour cell population.
[b]Values in parentheses are 95% confidence limits, determined using standard errors. When the ranges of 95% confidence limits showed no overlap between two values, the difference between the two values were significant ($p<0.05$) based on a χ^2 test.

pimonidazole-unlabelled cells and the whole cell fraction in both the Q and total cell populations, were efficiently reduced. Moreover, the capacity to recover from radiation-induced damage in both the Q and total cell populations as a whole and both the pimonidazole-unlabelled and the whole cell fraction of the Q and total cell populations was remarkably reduced (Tables 2 and 4). These findings, including newly elucidated characteristics concerning the response of the Q cell population and pimonidazole-unlabelled cell fraction in the total and Q cell populations, potentially reveal some reliable advantage of high-LET radiation over low-LET radiation in terms of controlling the CSCs or tumour clonogens that are thought to be resistant to cytotoxic treatment for solid tumours.

In boron neutron capture therapy (BNCT), the cellular distribution of ^{10}B from BSH is thought to be mostly dependent on the diffusion of the drug, whereas that from BPA is more dependent on the ability of the cells to take up ^{10}B [19]. Further, Q cell populations have been shown to have a much larger HF than total cell populations [2], and hypoxic cells are thought to exhibit less uptake ability than aerobic cells [1]. Therefore, it follows that Q cells have a lower uptake capacity than the total cell population, and that the distribution of ^{10}B from ^{10}B-carriers into Q cells is more dependent on the diffusion of the drugs than on the uptake ability of the cells. Tables 3 and 5 show that the distribution of ^{10}B in the tumour from BSH relies mostly on passive diffusion, whereas that from BPA relies on uptake capacity in tumour via active transport, the former resulting from a greater effect on Q cells, and the latter from a greater effect on the pimonidazole-unlabelled cell fraction and the total tumour cell population. In BNCR, when a ^{10}B-carrier, especially BPA, is employed, the difference in radiosensitivity, not only between total and Q cell populations as a whole but also between pimonidazole-unlabelled cells and the whole cell fraction of the Q and total cell populations, is rather extended compared with the case of disuse of ^{10}B-carrier. Consequently, without a reliable method of delivering a high enough amount of ^{10}B into target tumour cells efficiently irrespective of intratumour microenvironmental conditions including oxygenation status, it is hard to conclude that BNCT in combination with a ^{10}B-carrier can overcome the resistance to cytotoxic treatment of CSCs or tumour clonogens. Also in BNCT, compared with reactor neutron beam irradiation only, Q cells have been shown to have significantly less radiosensitivity than the total cell population when a ^{10}B-carrier, especially BPA, is employed (Table 7) [1, 2, 20]. Thus, more Q cells can survive BNCT than P cells (Figures 2 and 3, Table 7).

In the present study, the pimonidazole-unlabelled (and probably oxygenated) cell fraction showed a greater recovery capacity than the Q cell population as a whole. However, although there is similarity between the pimonidazole-unlabelled Q cell fraction and CSCs or tumour clonogens in terms of quiescent status and enhanced recovery capacity, CSCs or tumour clonogens are thought to exist under rather hypoxic conditions [15–17]. In the future, using human tumour cell lines, the characteristics of the intratumour Q cell population in connection with those of CSCs or tumour clonogens also have to be analysed.

References

1. Vaupel P. Tumor microenvironmental physiology and its implications for radiation oncology. Semin Radiat Oncol 2004;206:198–206.
2. Masunaga S, Ono K. Significance of the response of quiescent cell populations within solid tumors in cancer therapy. J Radiat Res 2002;43:11–25.
3. Masunaga S, Ono K, Suzuki M, Kinashi Y, Takagaki M. Radiobiologic significance of apoptosis and micronucleation in quiescent cells within solid tumors following γ-ray irradiation. Int J Radiat Oncol Biol Phys 2001;49:1361–8.
4. Ljungkvist AS, Bussink J, Rijken PF, Raleigh JA, Denekamp J, Van Der Kogel AJ. Changes in tumor hypoxia measured with a double hypoxic marker technique. Int J Radiat Oncol Biol Phys 2000;48:1529–38.
5. Hada M, Georgakilas AG. Formation of clustered DNA damage after high-LET irradiation: a review. J Radiat Res 2008;49:203–10.
6. Ahmed RS, Kim RY, Duan J, Meleth S, De Los Santos JF, Fiveash JB. IMRT dose escalation for positive para-aortic lymph nodes in patients with locally advanced cervical cancer while reducing dose to bone marrow and other organs at risk. Int J Radiat Oncol Biol Phys 2004;60:505–12.
7. Wulf J, Haedinger U, Oppitz U, Thiele W, Mueller G, Flentje M. Stereotactic radiotherapy for primary lung cancer and pulmonary metastases: a noninvasive treatment approach in medically inoperable patients. Int J Radiat Oncol Biol Phys 2004;60:186–96.
8. Masunaga S, Ono K, Suzuki M, Nishimura Y, Kinashi Y, Takagaki M, et al. Radiosensitization effect by combination with paclitaxel *in vivo* including the effect on intratumor quiescent cells. Int J Radiat Oncol Biol Phys 2001;50: 1063–72.
9. Hall EJ, Giaccia AJ. Radiosensitivity and cell age in the mitotic cycle. In: Hall EJ, Giaccia AJ, eds. Radiobiology for the radiologist. 7th edn. Philadelphia, PA: Lippincott Williams & Wilkins; 2012. pp. 54–66.

10. Masunaga S, Ono K, Sakurai Y, Takagaki M, Kobayashi T, Kinashi Y, et al. Evaluation of apoptosis and micronucleation induced by reactor neutron beams with two different cadmium ratios in total and quiescent cell populations within solid tumors. Int J Radiat Oncol Biol Phys 2001;51:828–39.
11. Kobayashi T, Kanda K. Microanalysis system of ppm-order ^{10}B concentrations in tissue for neutron capture therapy by prompt γ-ray spectrometry. Nucl Instrum Methods 1983;204: 525–31.
12. Sakurai Y, Kobayashi T. Characteristics of the KUR Heavy Water Neutron Irradiation Facility as a neutron irradiation field with variable energy spectra. Nucl Instr Meth A 2000;453:569–96.
13. Kobayashi T, Sakurai Y, Kanda K, Fujita Y, Ono K. The remodeling and basic characteristics of the heavy water neutron irradiation facility of the Kyoto University Research Reactor, mainly for neutron capture therapy. Nucl Tech 2000;131:354–78.
14. Snyder WS, Cook MJ, Nasset ES, Karhausen LR, Parry Howells G, Tipton I. Gross and elemental content of reference man. In: Snyder WS, ed. Report of the task group on reference man. Oxford, UK: Pergamon Press; 1975. pp. 273–324.
15. O'Brien CA, Kreso A, Dick JE. Cancer stem cells in solid tumors: an overview. Semin Radiat Oncol 2009;19: 71–6.
16. Hill RP, Marie-Egyptienne DT, Hedley DW. Cancer stem cells, hypoxia and metastasis. Semin Radiat Oncol 2009;19: 106–11.
17. Diehn M, Cho RW, Clarke MF. Therapeutic implications of the cancer stem cell hypothesis. Semin Radiat Oncol 2009;19:78–85.
18. Hamada N, Imaoka T, Masunaga S, Ogata T, Okayasu R, Takahashi A, et al. Recent advances in the biology of heavy-ion cancer therapy. J Radiat Res 2010;51:365–83.
19. Soloway AH, Hatanaka H, Davis MA. Penetration of brain and brain tumor. VII. Tumor-binding sulfhydryl boron compounds. J Med Chem 1967;10:714–17.
20. Vaupel P, Kallinowski F, Okunieff P. Blood flow, oxygen and nutrient supply, and metabolic microenvironment of human tumours: a review. Cancer Res 1989;49:6449–65.